# Quantifying isolated pore space in geological barrier materials

(Max) Qinhong Hu, Qiming Wang, Prince Oware, Tristan Tom, Yukio Tachi, Yuta Fukatsu, Jan Ilavsky, Jonathan Almer, Jun-Sang Park

University of Texas at Arlington; Japan Atomic Energy Agency; Argonne National Laboratory

**PRESENTED AT:**

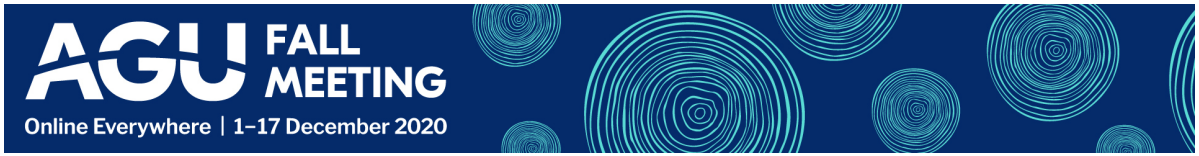

# RATIONAL AND EARLY WORK

**Historical Evolution of Major Research Thrusts in the Environment, Energy, and Resources Studies**

- Air and surface water contamination (1950s–1980s)
- Environmentalism movement (since 1960s)
- Soil contamination (1960s–present)
- Geothermal energy exploitation (1974–present)
- Tight sands and coalbed methane (1976–present)
- Geological repository of high-level nuclear waste (1978–present)
- Groundwater remediation and Superfund (1980–present)
- Carbon sequestration (1997–present)
- Petroleum production in shale gas and oil reservoirs (1981; 2008–present)
- Gas (methane) hydrate (2005–present)

involves clay materials & fractured media

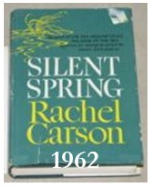




UNIVERSITY OF TEXAS-ARLINGTON

# Nuclear Power Plants Worldwide

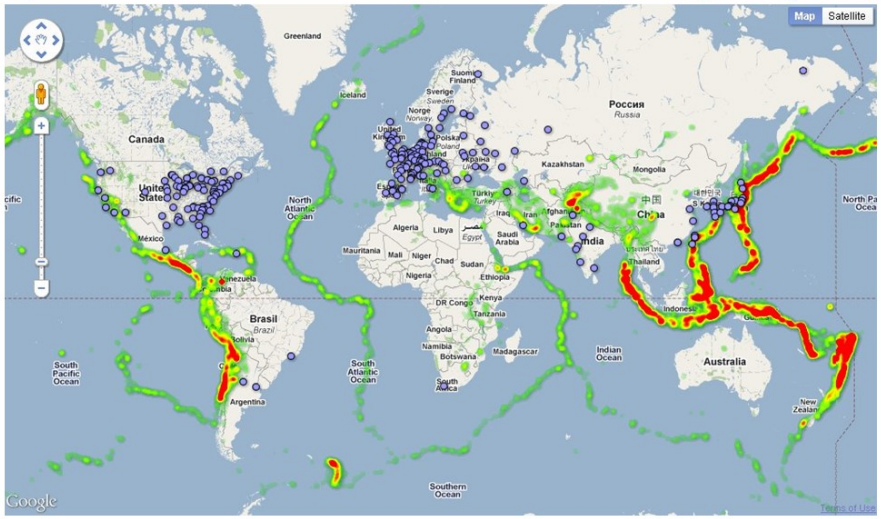


- ~35 countries
- 449 nuclear power reactors in operation
- 53 reactors under construction
- 5% of world energy and 15% of the world's electricity

http://www.iaea.org/pris/Home.aspx

http://www.targetmap.com/viewer.aspx?reportId=4850

UNIVERSITY OF TEXAS-ARLINGTON

**Annual production of spent nuclear fuel: 10,000 MT**

# Nuclear Power and Geological Repository in Major Countries

| Country | Operating plants in 2010 (2019) | Nuclear electricity generation in 2006 (2019) (billions kWh) | Nuclear electricity reliance (%) | Nuclear electricity of world total (%) | Projected repository operation |
|---|---|---|---|---|---|
| Belgium | 7 (7) | 44.3 (41.3) | 54 (47.6) | 1.7 (1.6) | between 2035–2080 |
| Canada | 18 (19) | 92.4 (95.5) | 18 (14.9) | 3.5 (3.8) | after 2034 |
| China | 11 (48) | 51.8 (348) | 2.1 (4.9) | 1.9 (13.8) | at earliest 2040 |
| Czech Republic | 6 (6) | 24.5 (28.6) | 32 (35.2) | 0.9 (1.1) | after 2030 |
| Finland | 4 (4) | 22 (22.9) | 30 (34.7) | 0.8 (0.9) | Olkiluoto in 2020; construc. in 2004; license in 2015; emplacement in 2023 |
| France | 59 (56) | 429 (380) | 76 (70.6) | 16 (15.0) | by 2025 |
| Germany | 17 (6) | 159 (0) | 28 (0) | 6.0 (0) | no projected date |
| India | 18 (22) | 15.6 (40.7) | 2.0 (3.2) | 0.6 (1.6) | TBD |
| Japan | 53 (33) | 292 (65.6) | 25 (7.5) | 11 (2.6) | at earliest 2035 |
| Korea (South) | 20 (24) | 141 (137) | 36 (26.2) | 5.3 (5.5) | TBD |
| Russia | 31 (38) | 144 (209) | 17 (19.7) | 5.4 (8.3) | after 2025 |
| Slovakia | 4 (4) | 16.6 (15.4) | 56 (53.9) | 0.6 (0.61) | TBD |
| Spain | 8 (7) | 57.4 (55.9) | 18 (21.4) | 2.2 (2.2) | TBD |
| Sweden | 10 (7) | 65.1 (55.9) | 42 (21.4) | 2.4 (2.2) | Forsmark, license applied in 2011 |
| Switzerland | 5 (4) | 26.4 (16.6) | 39 (23.9) | 1.0 (0.66) | after 2050 |
| Ukraine | 15 (15) | 84.8 (83.0) | 47 (53.9) | 3.2 (3.3) | after 2020 |
| United Kingdom | 19 (15) | 69.2 (51.0) | 13 (15.6) | 2.6 (2.0) | TBD |
| United States | 104 (95) | 787 (809) | 20 (19.7) | 30 (32.0) | Indefinite after 2008 |

UNIVERSITY OF TEXAS-ARLINGTON

# Geological Repository: Barrier (Host Rocks and Buffer) Materials

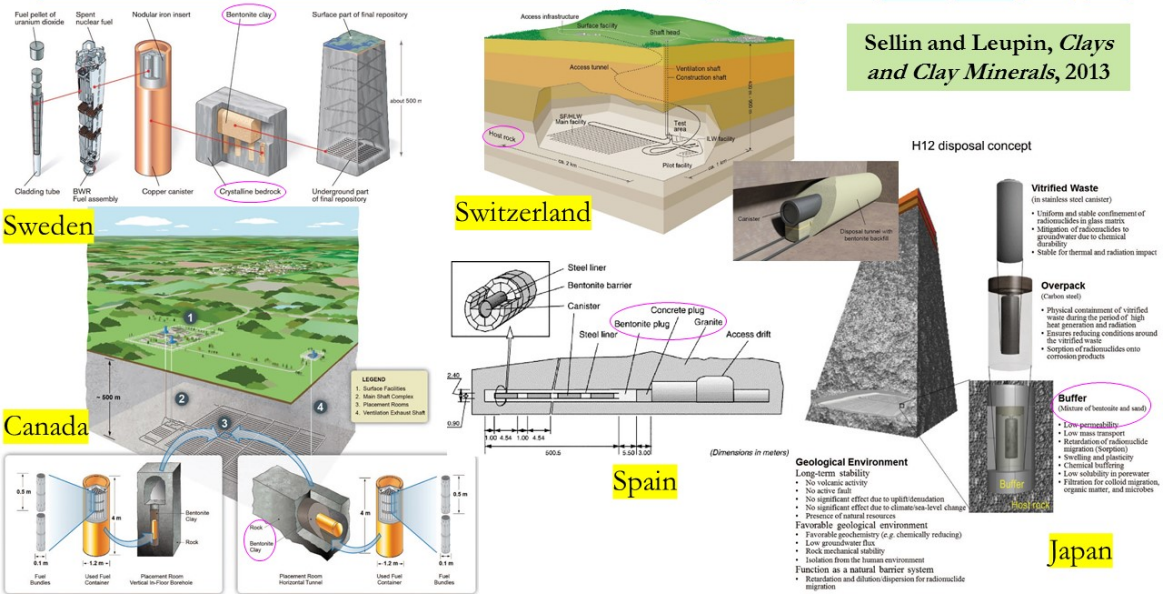


# Las Vegas, Nevada Test Site and Yucca Mountain

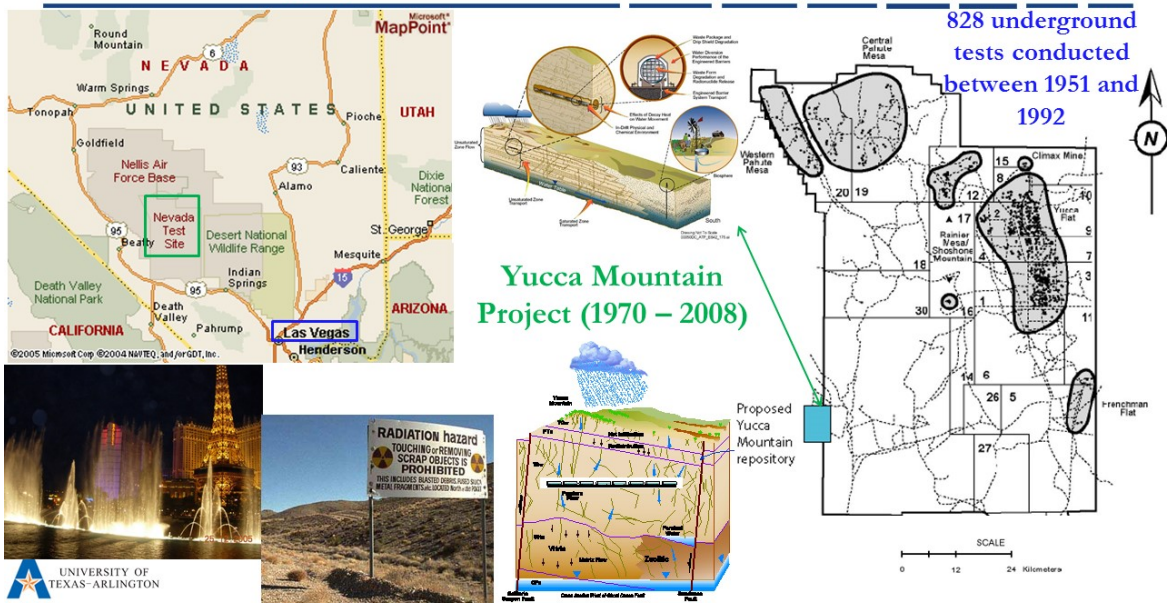

## Earlier Fracture-Matrix Interaction Studies

Field observation (preferential flow in a fracture network) of dye distribution in unsaturated fractured tuff at Yucca Mt.

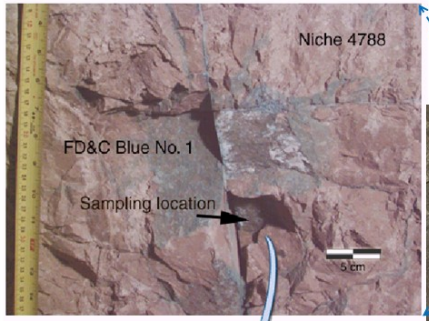


Exploratory Studies Facility (ESF); 1997

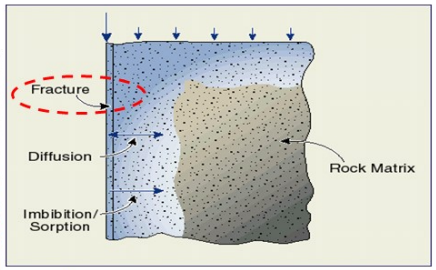


Rock milling in 1998

My work on fracture-matrix interaction starts with this rock

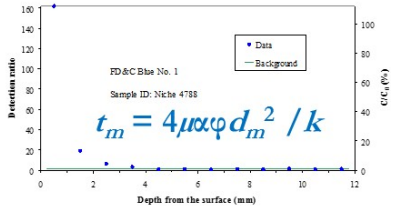


UNIVERSITY OF TEXAS-ARLINGTON

Hu et al., JCH, 2001; VZJ, 2002

## Imbibition in Fractured Rock: Sorptivity and Permeability

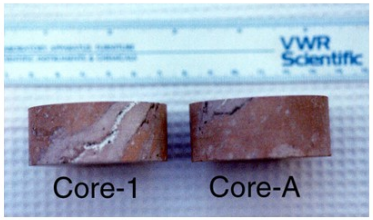


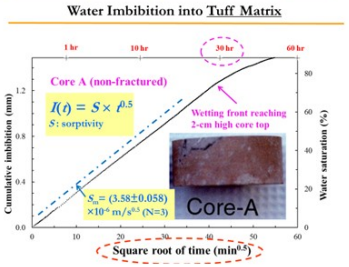



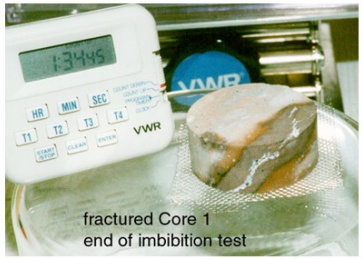


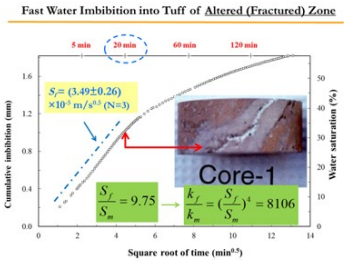


UNIVERSITY OF TEXAS-ARLINGTON

Hu et al., JH, 2001; VZJ, 2004

# Laboratory Tracer Tests and Penetration Delineation

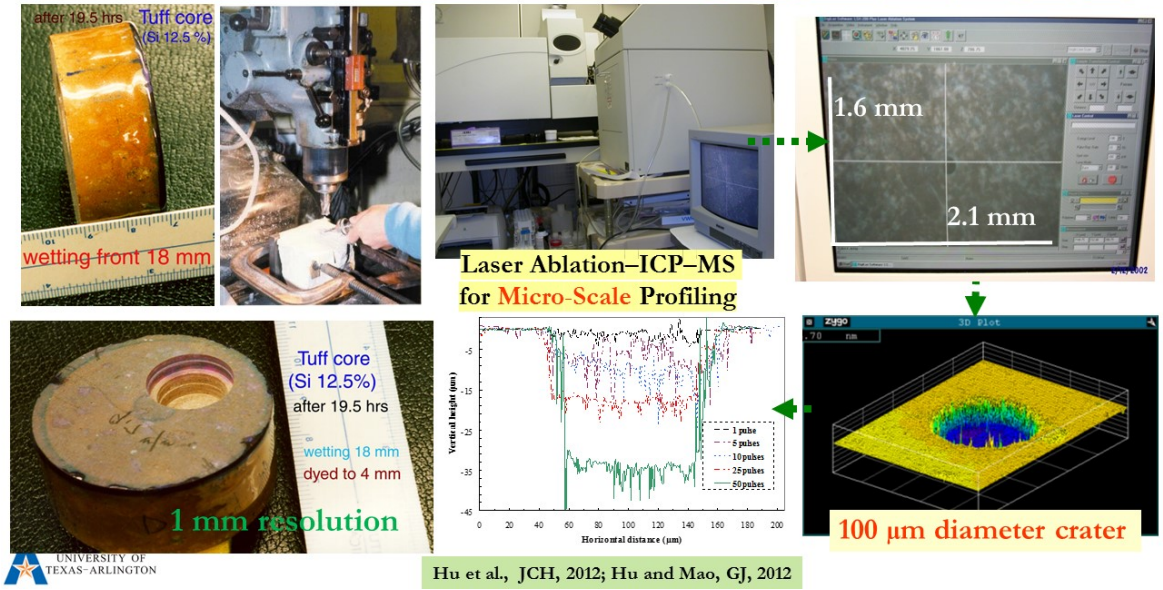


UNIVERSITY OF TEXAS-ARLINGTON

Hu et al., JCH, 2012; Hu and Mao, GJ, 2012

# SAMPLES AND METHODOLOGIES

## A Variety of Generic Geological Media: Host Rocks and Barrier Materials

| Sample | Topopah Spring Welded Tuff | Marcellus Shale | Mancos Shale | Wolfcamp Shale | Salt Rock | Cement / Concrete |
|---|---|---|---|---|---|---|
| Source | Yucca Mtn., NV | Centre County, PA | San Juan Co., NM | Midland County, TX | Carlsbad, NM | LLNL; EPA |

| Sample | Gray Chalk | Wakkanai Mudstone | Boom Clay | Grimsel Granodiorite | Granite | Opalinus Clay |
|---|---|---|---|---|---|---|
| Source | Negev Desert, Israel | Horonobe Underground Res. Center, Hokkaido, Japan | The HADES Underground Res. Lab., Belgium | Grimsel, Switzerland | Stripa mine, Sweden | Mt. Terri Underground Research Laboratory, Switzerland |

| Sample | Silica Sand | Berea Sandstone | Na-rich Montmorillonite | Illite | Kaolin | Chlorite |
|---|---|---|---|---|---|---|
| Source | Ottawa, IL | Berea Quarry, OH | Crook County, WY | Silver Hill, MT | Twiggs County, GA | El Dorado County, CA |

UNIVERSITY OF TEXAS-ARLINGTON

DOE-Nuclear Energy University Program: "Reduced diffusion and enhanced retention of multiple radionuclides from pore structure characterization of barrier materials for enhanced repository performance"

## Pore Structure: Geometry and Topology

Percolation theory: the mathematics of how macroscopic properties emerge from local (microscopic) connections

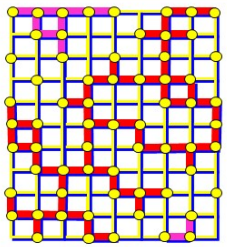

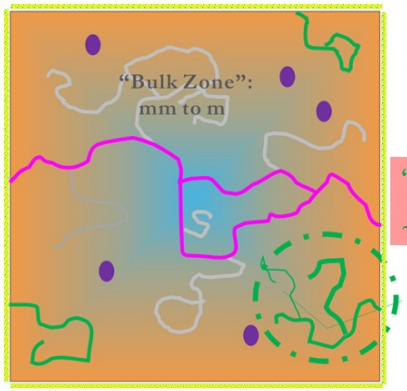


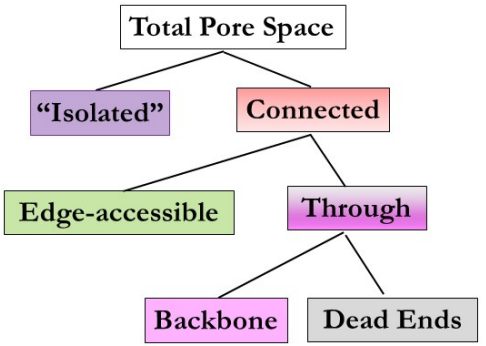


for mudrock

Hu et al., JGR, 2015

Effective porosity/Total porosity ($\phi_e / \phi$)

"Surface Zone": ~70%

"Bulk Zone": ~0.1%

## Multiple Approaches to Studying Pore Structure (Geometry and Topology)

- Vacuum saturation, liquid displacement, pycnometry, and enveloping methods of gas or hydrophilic / hydrophobic fluids (DIW; API brine; n-decane; toluene; isopropyl alcohol IPA; tetrahydrofuran THF; dimethylformamide DMF; crude oil) for fluid-accessible effective porosity of a range of sample sizes (μm – 10 cm)
- Fluid (DIW; API brine; n-decane; IPA) and tracer imbibition (bedding direction; initial fluid saturation; HPHT)
- Edge-accessible porosity after tracer vacuum-saturation and high-pressure intrusion
- Liquid and gas diffusion, under ambient and high-pressure / high-temperature conditions
- Mercury Intrusion Porosimetry
- Low-pressure gas adsorption isotherm and hysteresis
- Water vapor adsorption isotherm and hysteresis
- Nuclear Magnetic Resonance Cryoporometry
- Ar ion milling Field Emission-SEM (FE-SEM) and QEMSCAN (Quantitative Evaluation of Materials by Scanning) mapping, correlated with tracer mapping to study Dalmatian wettability and connectivity of shale pore systems
- 2-D imaging/mapping after Wood's metal impregnation
- Microtomography (high-resolution, synchrotron, nano-CT)
- Focused Ion Beam/SEM (FIB-SEM) imaging
- Small-Angle Neutron Scattering (U)SANS
- Small-Angle X-Ray Scattering (U)SAXS
- Pore-scale network modeling
- Physics-based production decline analyses

UNIVERSITY OF TEXAS-ARLINGTON

Hu et al., Hedberg Conference, 2010

## A Range of Sample Sizes for Different Tests

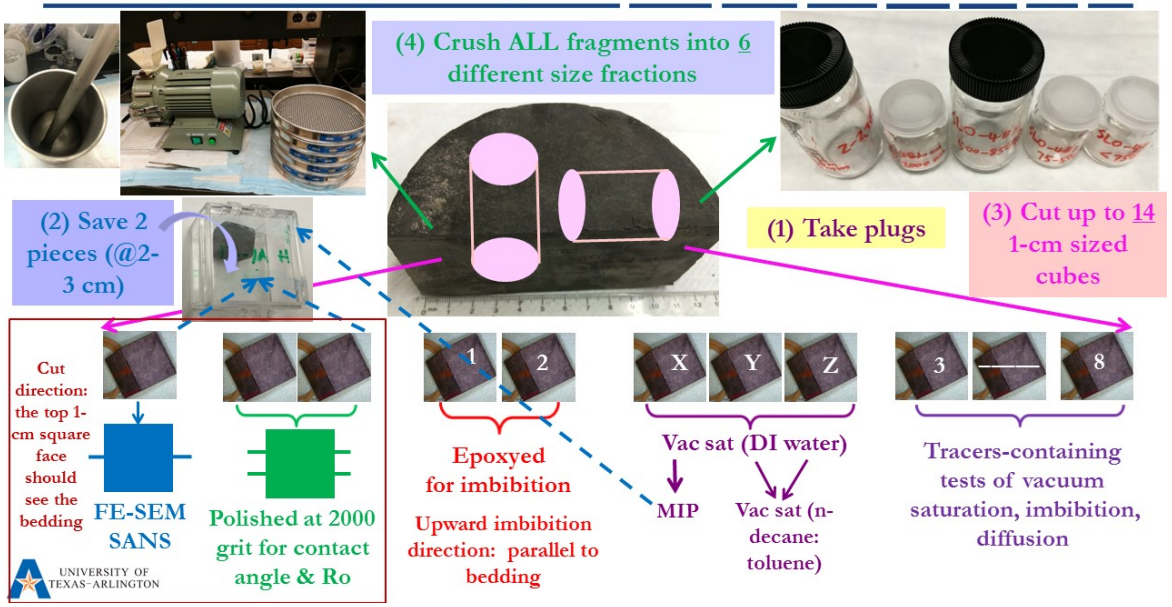

# A Range of Sample Sizes for Pore Structure Characterization

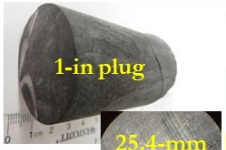



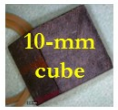


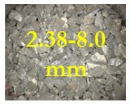



| Size designation | Sieve mesh | Size fraction (diameter) | Equivalent spherical dia. (μm) | Equivalent spherical dia. (mm) |
|---|---|---|---|---|
| Cylinder / Plug | | 2.54 cm dia.; any height (e.g., 3 cm) | *(24394)* | *(24.39)* |
| Cube | | 1.0 cm | 9086 | 9.086 |
| Size X | 8 mm to #8 | 2.38 - 8.0 mm | 5180 | 5.180 |
| GRI+ | #8 to #12 | 1.70 - 2.38 mm | 2030 | 2.030 |
| Size A | #12 to #20 | 841 - 1700 μm | 1271 | 1.271 |
| GRI | #20 to #35 | 500 - 841 μm | 671 | 0.671 |
| Size B | #35 to #80 | 177 - 500 μm | 339 | 0.339 |
| Size C | #80 to #200 | 75 - 177 μm | 126 | 0.126 |
| Powder | <#200 | < 75 μm | < 75 | < 0.075 |
| Size D | #200 to #625 | 20 - 75 μm | 47.5 | 0.0475 |
| Size E | <#635 | <20 μm | <20 | <0.02 |






UNIVERSITY OF TEXAS-ARLINGTON

**GRI: Gas Research Institute**

# RESULTS: PYCNOMETRY, POROSIMETRY, AND TRACER MAPPING

## Helium Pycnometry for Grain Density: Envelop Method for Bulk Density

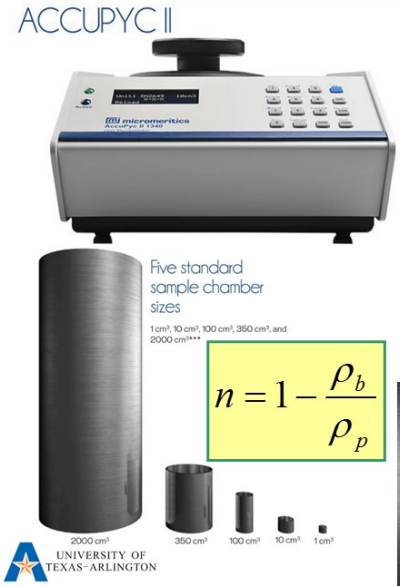


$$n = 1 - \frac{\rho_b}{\rho_p}$$


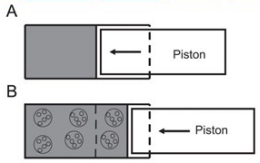


- Envelop media: 20-75 μm solid quartz
- Measurable sample sizes: plugs to Size C

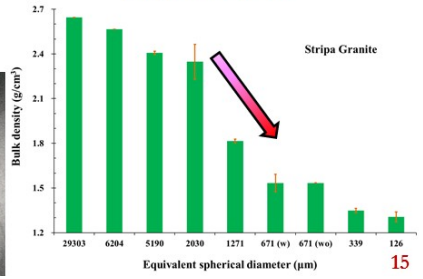


15

# Multiple nm-μm Pore Systems of Mudrock

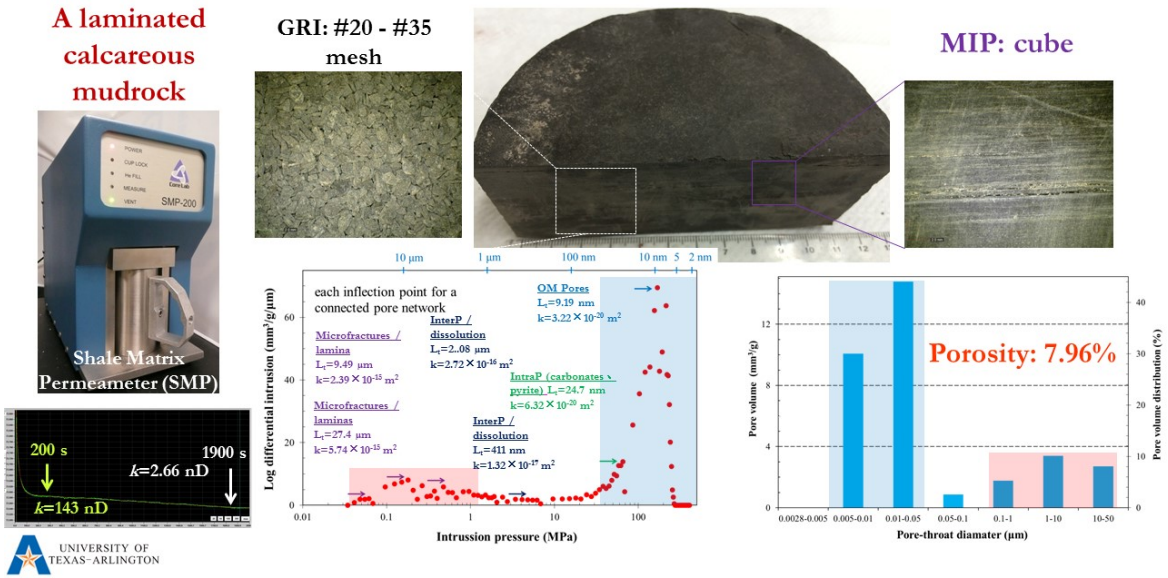


# Pore-Throat Size Distribution and Pore Connectivity

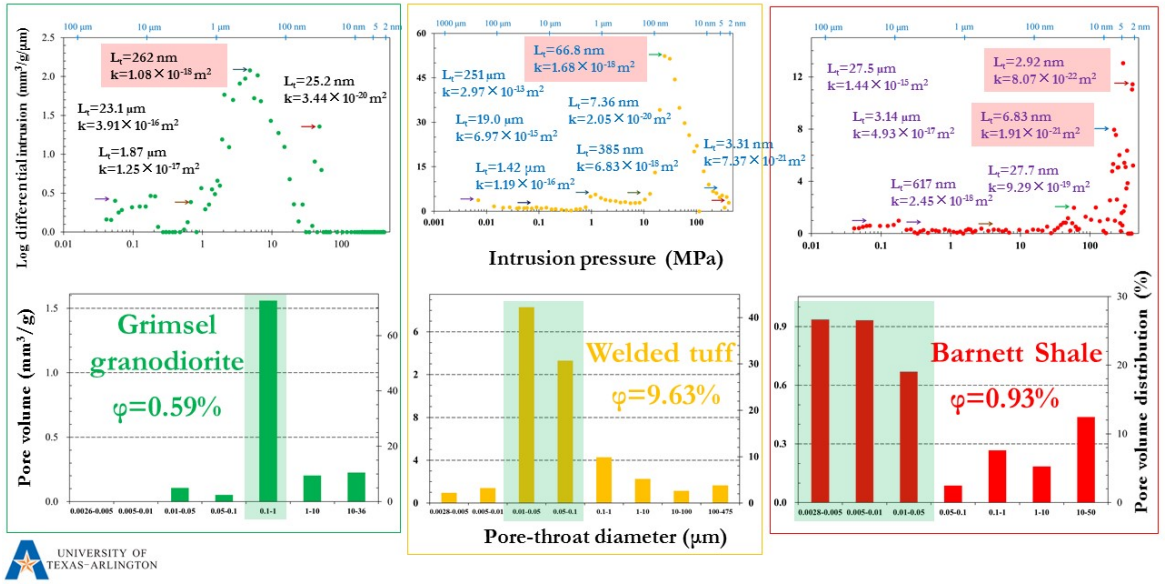

## MIP Analyses of Pore Structure and Network: Barnett Shale

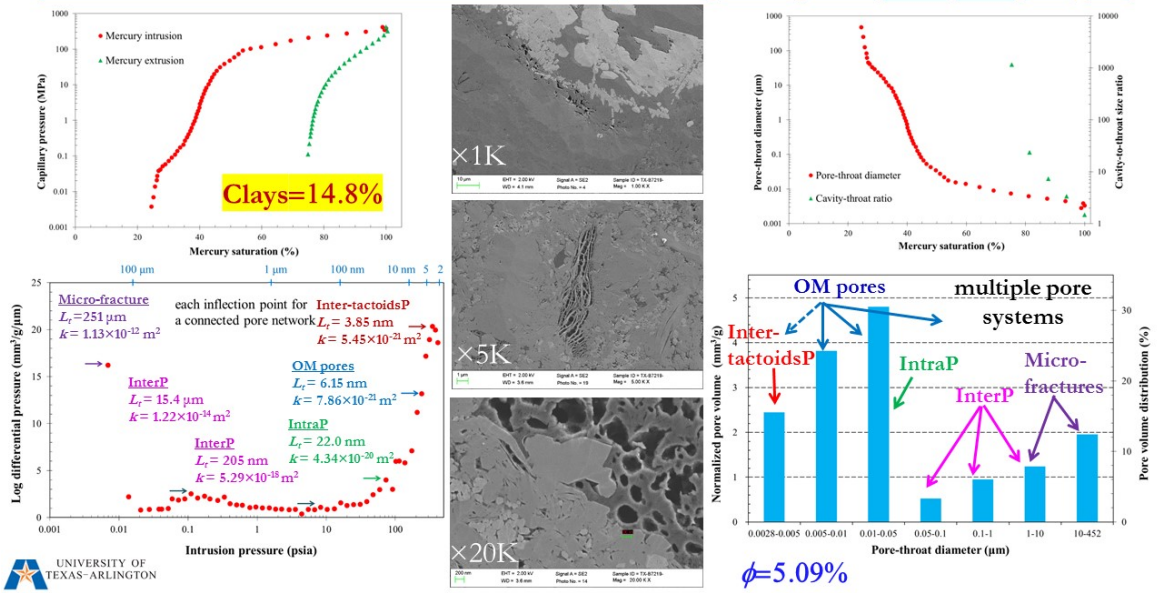


## Clay Structure and Pore Space at Different Scales

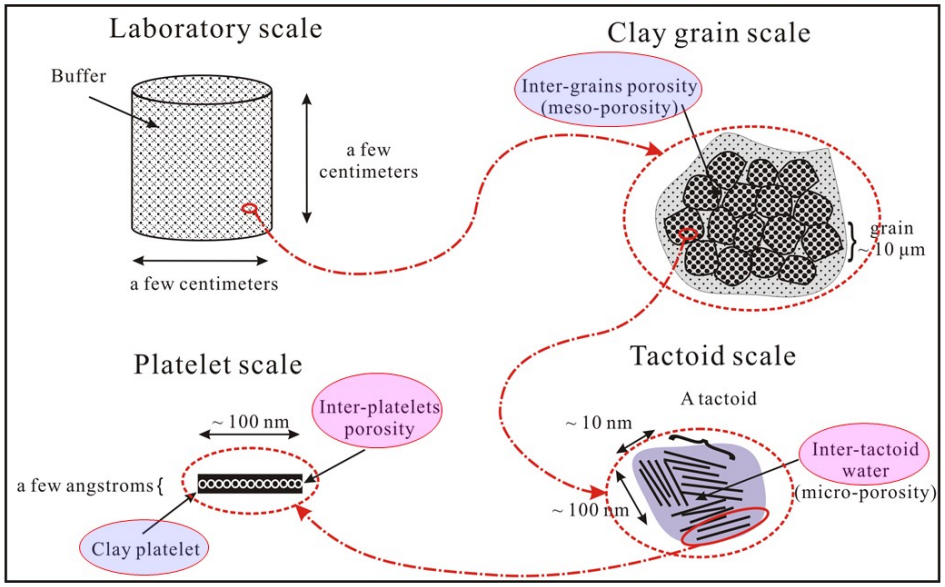

# Wettability-based Fluids and Tracers

- Groundwater simulate [5 mM $Ca(NO_3)_2$; water-wet]
  - ✓ $I^-$, $Br^-$ (0.181 nm)
  - ✓ $ReO_4^-$ (0.553 nm), $MoO_4^{2-}$ ($RuO_4^-$, $SeO_4^{2-}$, $CrO_4^{2-}$)
  - ✓ 0.313 nm $Cs^+$, 0.211 nm $Co^{2+}$, 0.245 nm $Sm^{3+}$ ($Eu^{3+}$)
- API brine (8 wt% NaCl+2 wt% $CaCl_2$) [water-wet]
  - ✓ $ReO_4^-$ (0.553 nm)
  - ✓ Anionic Sb-complex (0.89 nm)
  - ✓ Cationic Ru-complex (1.0 nm)
  - ✓ CdS nanoparticles (5–10 nm)
- n-decane: toluene [oil-wet]
  - ✓ Organic-I (1-iododecane)
  - ✓ Organic-Re [trichlorooxobis(triphenylphosphine)rhenium(V)]
  - ✓ $CeF_3$ nanoparticles (10–12 nm)
- IPA [zewittering]
  - ✓ Ru-complex (2.42 nm)

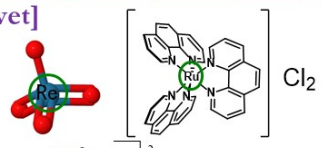


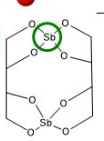

0.23 nm — 1.393 nm × 0.287 nm × 0.178 nm

$CH_3(CH_2)_8CH_2I$

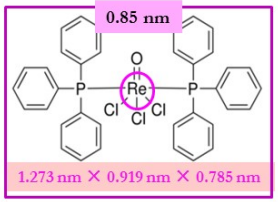


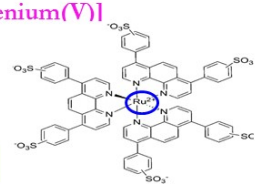

UNIVERSITY OF TEXAS-ARLINGTON

Hu et al., J. Nano. Nanotech., 2017

# Different Tracer Tests for Process-Level Understanding


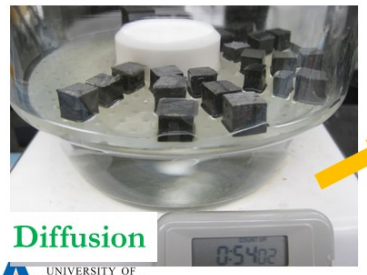


Laser Ablation-Inductively Coupled Plasma-Mass Spectrometry (LA-ICP-MS)

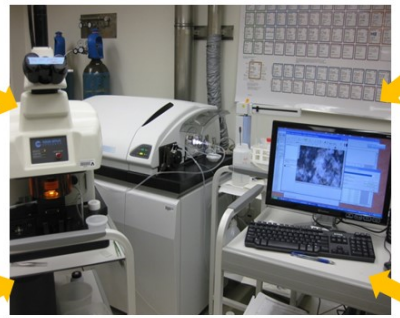

Hu et al., *VZJ*, 2004; *GJ*, 2012



UNIVERSITY OF TEXAS-ARLINGTON

# Unique Dual-Connectivity Zones of Mudrock: Multiple Evidence

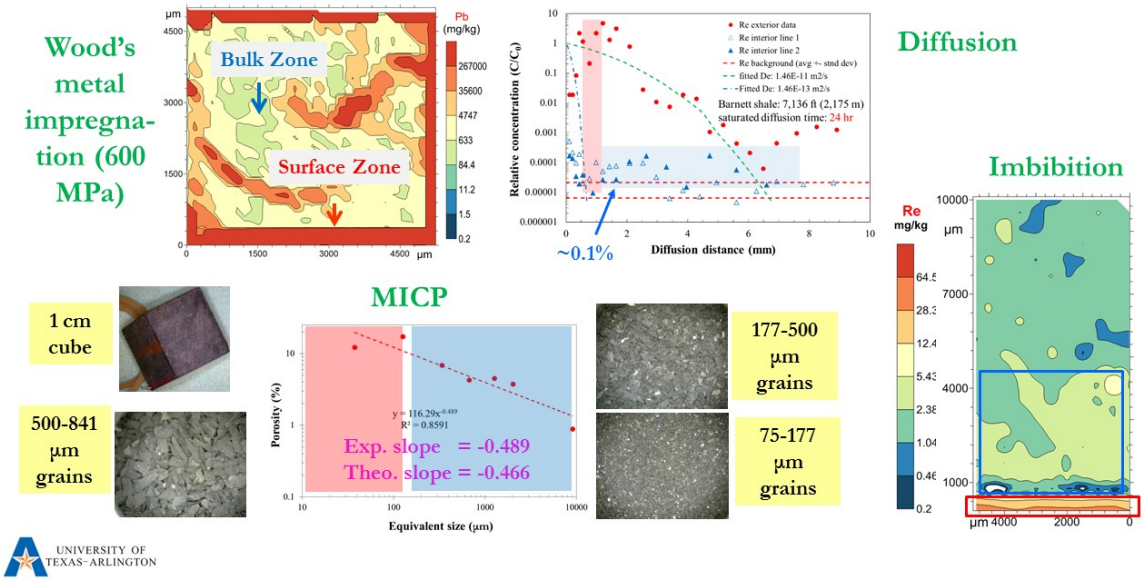

# RESULTS (SCATTERING) & CONCLUSIONS

## Small Angle Neutron Scattering (SANS)

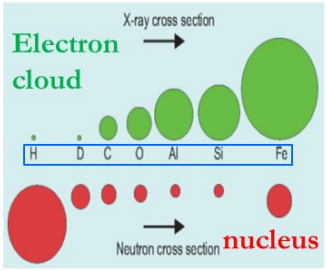


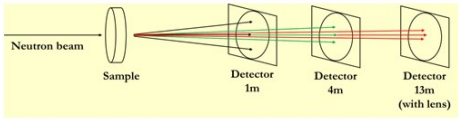


- Detect both connected and closed pores
- Obtain full-scale nm-μm pore diameters
- Quantify hydrophilic vs. hydrophobic pore space
- Investigate reservoir P-T condition

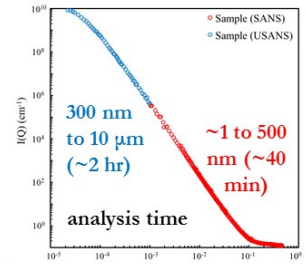


UNIVERSITY OF TEXAS-ARLINGTON

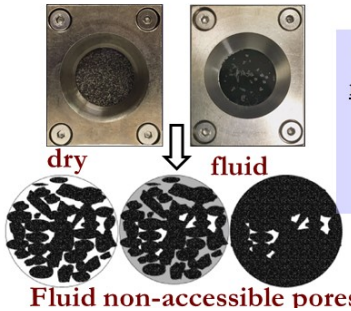


**Contrast matching**
d-$H_2O$
d-2DT
d-IPA

- Yang et al., Fuel, 2017
- Sun et al., IJCG, 2017
- Zhao et al., SR, 2017
- Zhang et al., MPG, 2019

## YMP Welded Tuff: (U)SANS and Other Results

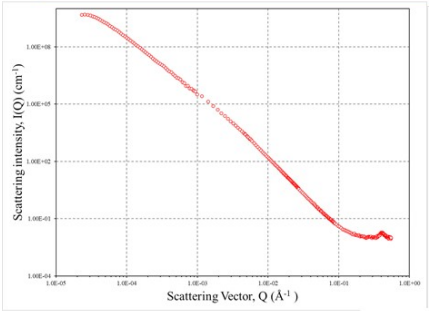


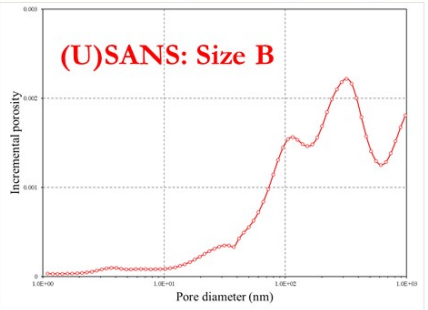


| Pore diameter | Porosity (%) |
|---|---|
| 1-2 nm | 0.02 |
| 2-50 nm | 0.61 |
| 50-100 nm | 0.71 |
| 100 nm-1 μm | 4.18 |
| Total | 5.52 |

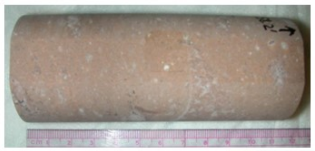

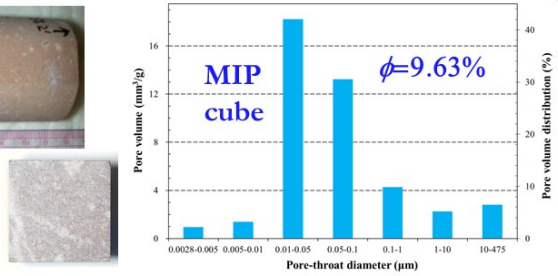


UNIVERSITY OF TEXAS-ARLINGTON

**FIP (cubes): 9.11±0.05%**

# Wolfcamp Shale: (U)SANS and Other Results

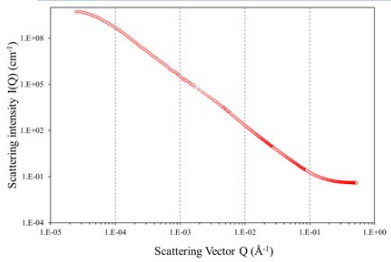


SANS: grains (177-500 μm)

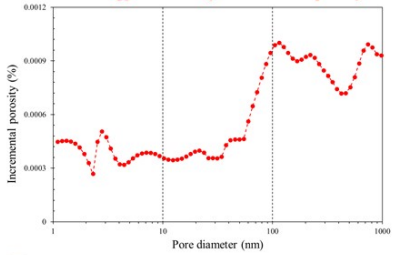


| Pore diameter (μm) | MIP (2.8 nm - 50 μm) | | SANS (1 nm - 20 μm) | | Pore body : cavity ratio |
|---|---|---|---|---|---|
| | Porosity (%) | Porosity distribution (%) | Porosity (%) | Porosity distribution (%) | |
| 0.0001-0.0028 | | | 0.459 | 10.5 | |
| 0.0028-0.005 | 0.783 | 16.4 | 0.239 | 5.49 | 0.33 |
| 0.005-0.01 | 1.05 | 22.1 | 0.28 | 6.45 | 0.29 |
| 0.01-0.05 | 1.00 | 20.9 | 0.66 | 15.1 | 0.72 |
| 0.05-0.1 | 0.365 | 7.64 | 0.553 | 12.7 | 1.7 |
| 0.1-1 | 1.57 | 33.0 | 2.17 | 49.8 | 1.5 |
| Total | 4.77 | | 4.35 | | |

FIP (cylinder & cubes) porosity: 2.93±0.15%

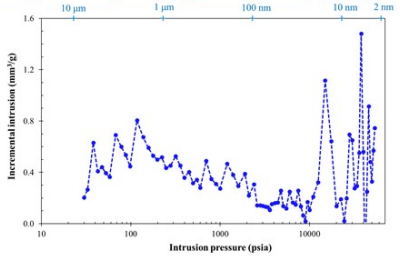


MIP: grains (177-500 μm)

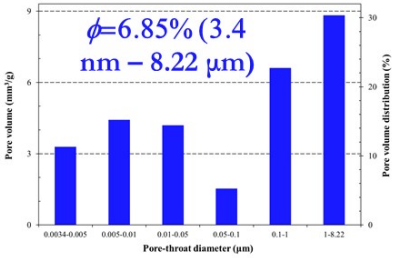


UNIVERSITY OF TEXAS–ARLINGTON

# Japan Wakkanai Mudstone: USANS and Other Results

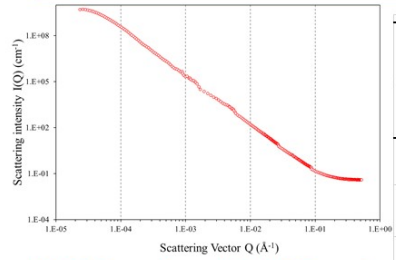


SANS: grains (177-500 μm)

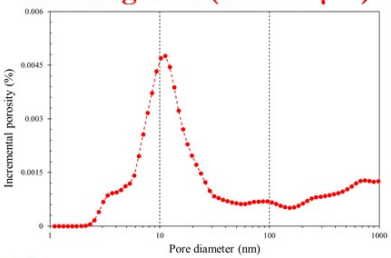


| Pore diameter (μm) | MIP (2.8 nm - 50 μm) | | SANS (1 nm - 20 μm) | | Pore body : cavity ratio |
|---|---|---|---|---|---|
| | Porosity (%) | Porosity distribution (%) | Porosity (%) | Porosity distribution (%) | |
| 0.0001-0.0028 | | | 0.063 | 0.710 | |
| 0.0028-0.005 | 0.0662 | 0.235 | 0.612 | 6.90 | 29.3 |
| 0.005-0.01 | 5.29 | 18.8 | 2.24 | 25.3 | 1.3 |
| 0.01-0.05 | 11.6 | 41.3 | 3.31 | 37.3 | 0.9 |
| 0.05-0.1 | 4.47 | 15.9 | 0.497 | 5.60 | 0.4 |
| 0.1-1 | 6.69 | 23.8 | 2.15 | 24.2 | 1.0 |
| Total | 28.1 | | 8.87 | | |

FIP (cylinders & cubes) porosity: 34.6±0.66%

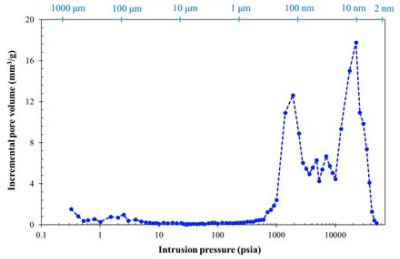


MIP: cube (1 cm)

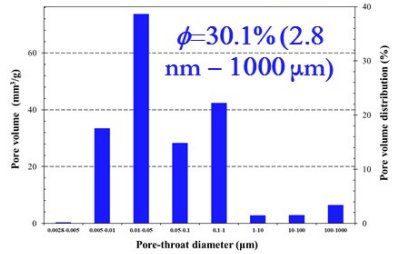


UNIVERSITY OF TEXAS–ARLINGTON

## X-ray Scattering Application

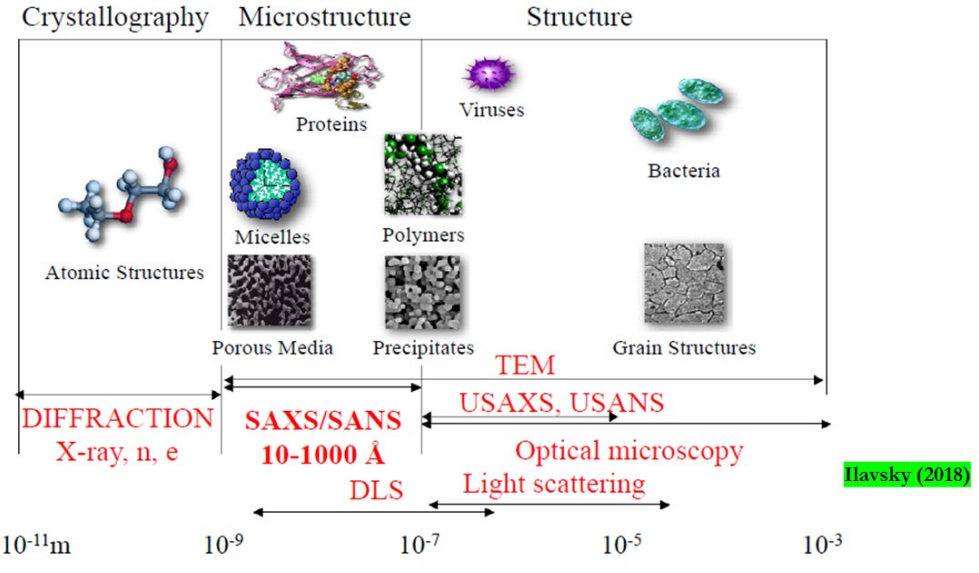


Ilavsky (2018)

UNIVERSITY OF TEXAS-ARLINGTON

## Advanced Photon Sources (APS)


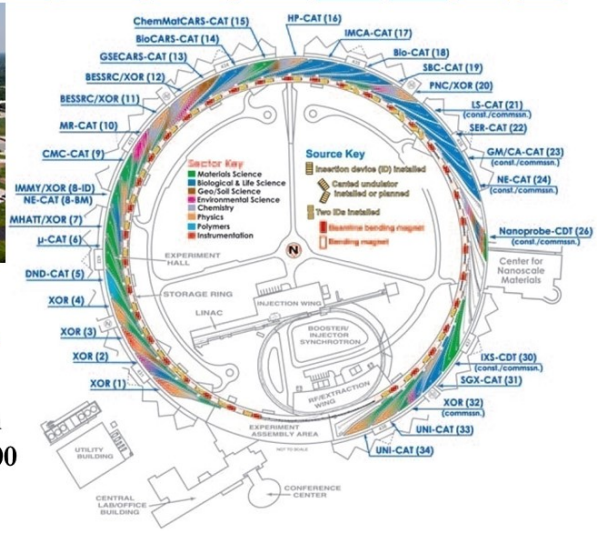


- 80-acre site; ~450 employees
- The brightest x-ray beams in the Western Hemisphere
- The largest of the 5 DOE light sources in terms of users per year for more than 5,000 (and growing) scientists from around the United States and the world

UNIVERSITY OF TEXAS-ARLINGTON

http://www.aps.anl.gov/

## 9-ID: USAXS/SAXS/WAXS

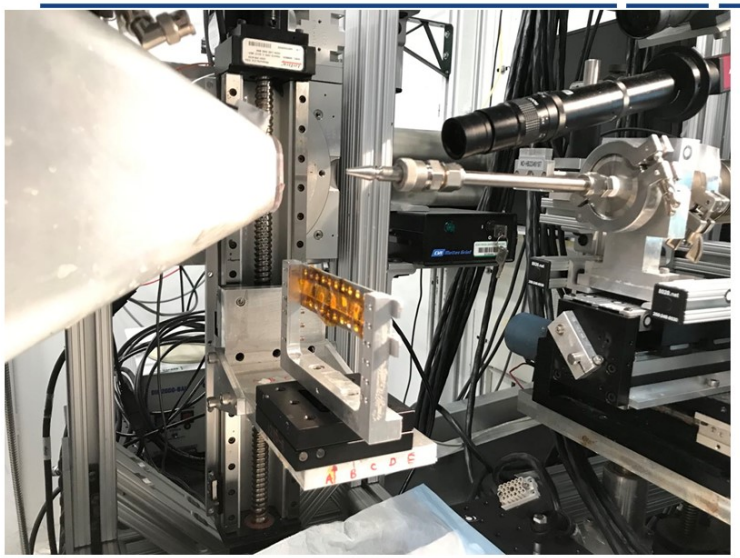

- Energy range: 10-24 keV
- Beam size:
- Analytical time: 4-5 min one position

"New user and joint SANS/SAXS proposals on pore connectivity studies of shale gas and oil reservoirs" (2 days of 9-ID, 8/2020)

Jan Ilavsky

UNIVERSITY OF TEXAS-ARLINGTON

https://youtu.be/-a9nD4W2ShQ

26

## Sample Preparation: Solid Form and Thickness

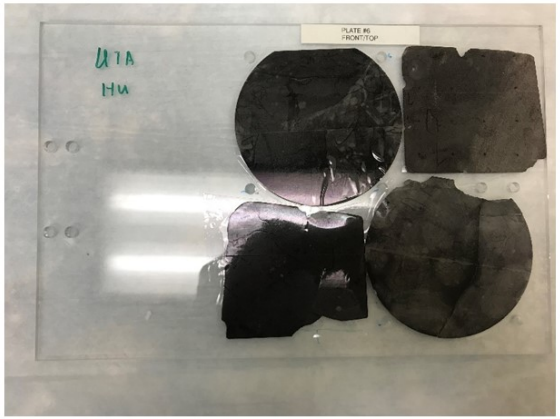

Whole core wafers: height= 0.5~0.8 mm

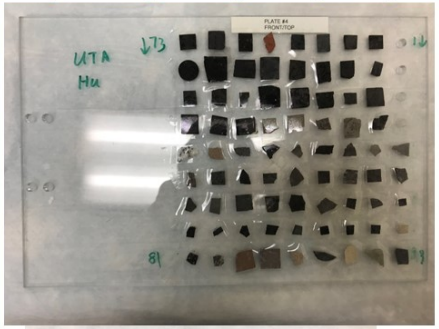

~1 cm wafer: height @ 0.5~0.8 mm

(Micro) Cuvettes: granular sample thickness @ 0.5, 1, and 4 mm

UNIVERSITY OF TEXAS-ARLINGTON

# High-Energy SAXS/WAXS at 1-1D

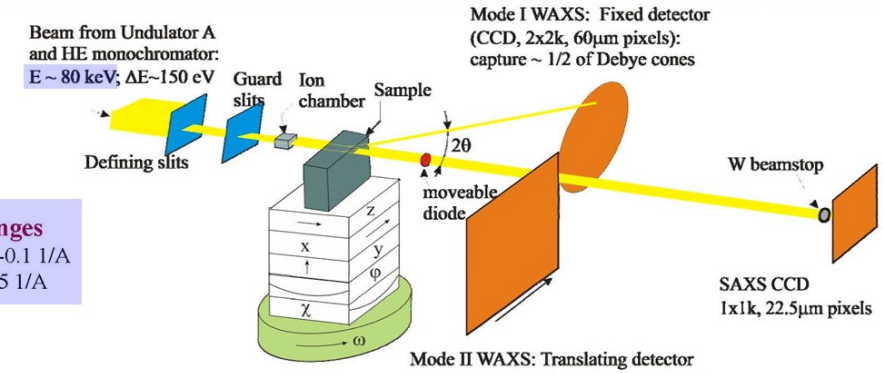


**Typical q-ranges**
- SAXS: 0.002-0.1 1/A
- WAXS = 0.2-5 1/A

**Features**
- *Direct* depth resolution to ~5μm with current pinhole setup
- Strong penetration ability: comparable to neutrons
- Perform WAXS,SAXS (and imaging) with little change in setup
- $t_{exposure}$ ~ 1-100 sec (both WAXS and SAXS)
- Plan to incorporate refractive-lens focusing optics (late 2004):
  - anticipate q(min) to ~ 0.0005 1/A
  - 1-D spatial resolution to ~1μm

✓ Jon Almer

✓ Jun-Sang Park

UNIVE TEXAS-.

# Sample Preparation: Form and Thickness

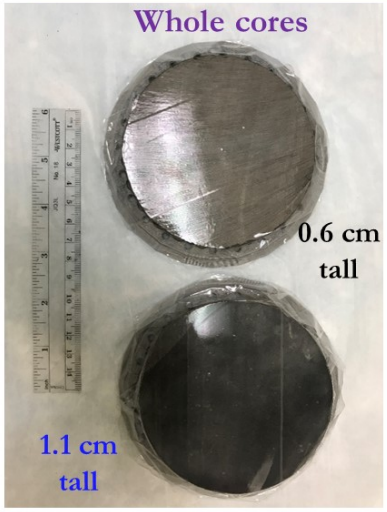


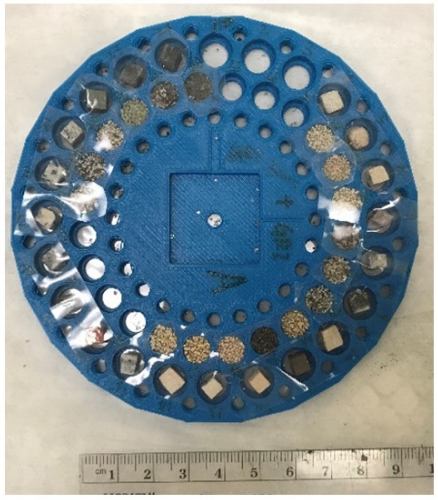

- granular
- non-granular


UNIVERSITY OF TEXAS-ARLINGTON

"New user and joint SANS/SAXS proposals on pore connectivity studies of shale gas and oil reservoirs" (2 days of 9-ID WAXS/SAXS/USAXS, 8/2020)

## Summary

- A variety of generic barrier materials are studied
- Dual connectivity zones are observed for mudrock
- Pore structure, especially pore connectivity, influences fluid flow and chemical transport in low-permeability media
- Limited pore connectivity will be conductive to enhanced diffusion and retention of radionuclides in barrier materials

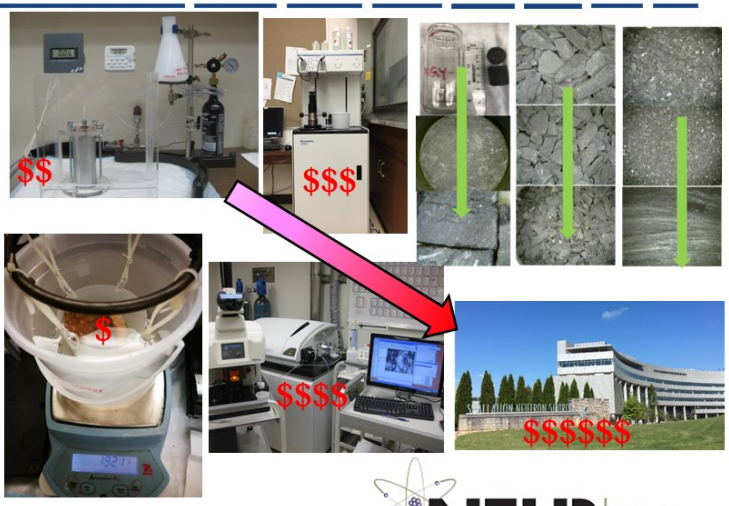


UNIVERSITY OF TEXAS-ARLINGTON

Japan Atomic Energy Agency

NEUP Nuclear Energy University Program
U.S. Department of Energy

## Acknowledgments

RPSEA Research Partnership to Secure Energy for America
ConocoPhillips
Japan Atomic Energy Agency
Sinopec
NEUP Nuclear Energy University Program
U.S. Department of Energy

USGS science for a changing world
Bureau of Economic Geology
New Mexico Tech
North Dakota Geological Survey
1895
Ohio Department of Natural Resources Geological Survey
Diamondback Energy
Vitruvian Exploration
Pennsylvania Geological Survey Est. 1836
element petroleum III, llc
Pioneer Natural Resources
Exxon
XTO Energy

Leibniz Universität Hannover
EMPA Materials Science & Technology
Iowa State University
Oak Ridge National Laboratory
NIST


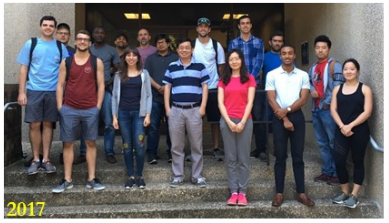



UNIVERSITY OF TEXAS-ARLINGTON

# ABSTRACT

Pore connectivity, a topological characteristic of pore structure, is oftentimes more important than the geometrical aspects in controlling fluid flow and mass transport in porous natural rocks as well as their associated utilities in energy and environmental stewardship. A different extent of pore connectivity can be reflected in the proportion of isolated pore space not connected to the surface of natural rocks. This work presents the multi-approach and multi-scale laboratory studies to investigating the proportion of isolated pore space of, and its resultant anomalous fluid flow and radionuclide movement in, generic geological barrier materials (clay sediment, crystalline rock, salt rock, shale, tuff). The samples include clay sediments of Wakkanai formation at Horonobe underground research center in Hokkaido of Japan, Opalinus clay of Mt. Terri Underground Research Laboratory as well as granodiorite from the Grimsel Test Site in Switzerland, salt rock from Waste Isolation Pilot Plant in New Mexico, various shales (Barnett, Eagle Ford and Wolfcamp from Texas), and welded tuff in Yucca Mountain in Nevada. Working with sample sizes from <75 μm to several centimeters, the experimental approaches include the independent quantification of both (1) surface-accessible pore space with various probing fluids (e.g., helium in expansion, water in vacuum saturation and nuclear magnetic resonance, mercury in intrusion porosimetry, nitrogen in gas physisorption, and Wood's metal in high-pressure impregnation and micron-scale tracer mapping using laser ablation-ICP-MS); and (2) total (both connected and isolated) porosity by small angle X-ray scattering. In summary, our evolving complementary approaches provide a rich toolbox for tackling the pore structure characteristics in geological barrier materials, and associated fluid flow & radionuclide transport, implicated in their long-term performance in natural and engineered systems of a nuclear waste repository.

Acknowledgements: This project was completed with funding provided by the Nuclear Energy University Program of Office of Nuclear Energy at the U.S. Department of Energy (award number DE-NE0008797) and Japan Atomic Energy Agency.